DOI: 10.19884/j.1672-5220.202403018

Hydrogen Sensing Characteristics of Gas Sensor Based on Pt/Graphene Composite

HOU Tianhao, PENG Yitian, DING Shuyang *
College of Mechanical Engineering, Donghua University, Shanghai 201620, China

Abstract: Graphene has exceptional electrical, optical and thermal properties, and is widely used to create thinner, lighter and faster sensors. In this study, graphene was fabricated by mechanically exfoliating on the SiO_2/Si substrate and the graphene field effect transistor (FET) was prepared by photolithography. Platinum (Pt) particles were doped on the surface of graphene by the hydrazine hydrate reduction method to endow a Pt/graphene sensor with gas-sensing properties. By being tested on a gas detection platform, the characteristics of the electrical (*I-V*) curves and resistance response curves were obtained in different hydrogen environments. The results show that the Pt/graphene sensor exhibits a high sensitivity to hydrogen at room temperature, with a resistance response rate of 33.35% at a hydrogen volume fraction of 1.00%. However, the sensitivity lifetime study shows an essential hysteresis in desorption process, which leads to gradually decreases in the resistance response rate. This research provides an improved production method of graphene-based gas sensors, which has a wide range of potential applications in aero-space industry.

Keywords: graphene; platinum (Pt) particle; hydrogen sensor; chemical adsorption
CLC number: TP212.9 **Document code**: A
Article ID: 1672-5220(2025)05-0485-09

Open Science Identity (OSID)

0 Introduction

Hydrogen, as an efficient and environmentally friendly energy source, is expected to be widely used in the future in a number of fields such as transport, construction and electricity[1]. However, there are certain safety hazards and risks involved in the production and application of hydrogen. Hydrogen is a colorless and odorless gas that is difficult for humans to identify, and excessive concentrations may cause asphyxiation[2-3]. Hydrogen molecules are extraordinarily small and diffuse through air at a very high rate, enabling them to permeate many materials and inflict irreversible damage[4]. Accurate detection of the hydrogen volume fraction is therefore essential, and it is one of the key ways to minimize potential safety risks.

Gas sensors are widely used for resistance-change detection because of their direct measurement principle, simple structure and low manufacturing cost[5-6]. Numerous studies have confirmed that reducing the dimensionality of a material can increase the sensitivity of a sensor by multiples or even orders of magnitudes[7-8]. Graphene is considered to be an innovative material that can enhance the performance of sensors due to its larger specific surface area and higher carrier migration rate[9-10]. Theoretical and experimental results show that intrinsic graphene has a high sensitivity and poor selectivity for a few gases[11]. Hydrogen adsorbed on unmodified graphene has a low adsorption energy and a low number of charge transfers, so unmodified graphene does not have sensitivity towards hydrogen[7,12]. In previous studies, to improve the sensitivity and selectivity of graphene sensors to hydrogen, graphene was usually used as a carrier for hydrogen-sensitive materials, and semiconducting metal oxides were doped on graphene[13-14], metals[15-17], polymers[18-19] and composite materials[20-24].

Platinum (Pt) is a common metal material for modification with a high sensitivity and selectivity to hydrogen. Hydrogen-modified Pt exhibits a higher resistivity than intrinsic Pt, making it better suited for resistance-based detection[25]. Pt/graphene composites made by Pt-modified graphene show many advantages in hydrogen detection. In theory, adjusting the metal structure at the nanoscale can maximize the sensitivity of metal-based gas sensors[26]. Yang et al.[27] explored the possibility of using Pt as a hydrogen sensor and confirmed the specific effect of the Pt sensor on the hydrogen sensing performance.

Graphene essentially exhibits a two-dimensional surface property with a extremely high carrier mobility[28-29], which makes graphene an ideal material for sensing[30-32]. In previous studies, researchers have verified the adsorption performance of NH_3 on the surface of Pt-modified graphene sheets[33] and the interaction mechanism of H_2S with Pt/graphene through the density functional theory (DFT) calculations[34]. The mechanism of Pt/graphene for gas detection was verified by the

Received date: 2024-03-28
Foundation item: National Natural Science Foundation of China (No. 51905090)
* Correspondence should be addressed to DING Shuyang, email: shuyangding@dhu.edu.cn
Citation: HOU T H, PENG Y T, DING S Y. Hydrogen sensing characteristics of gas sensor based on Pt/graphene composite[J]. *Journal of Donghua University (English Edition)*, 2025, 42(5): 485-493.

adsorption energy and charge transfer. Harley-Trochimczyk's research team[35] succeeded in creating a low-energy hydrogen sensor by loading functionalized Pt particle polysilicon onto graphene with a high specific surface area. At a hydrogen volume fraction of 0.01%, the sensitivity reached 1.6%; at a temperature of 90 ℃, the response and recovery times were relatively shortened, with a detection limit of 0.006 5%. Phan et al.[36] reported that Pt/palladium (Pd) alloy modified graphene hydrogen sensor had a wide hydrogen detection limit and high sensitivity. Under ambient conditions, the detection sensitivity of the hydrogen sensor was closely related to the hydrogen flow rate.

In this study, we prepare a graphene field effect transistor (FET) by using mechanically exfoliated graphene as a carrier. A Pt/graphene sensor is prepared by depositing Pt particles on the graphene surface with the hydrazine hydrate reduction method. The effect of Pt modification on the properties of graphene is investigated, the hydrogen detection characteristics under environmental conditions are explored, and the resistance response curves of the Pd/graphene sensor are compared. In addition, the basic principle of hydrogen adsorption and desorption is analyzed through the continuity test of the sensor and the resistance response curves.

1 Materials and Methods

1.1 Materials

Graphene was provided by Six Carbon Technology (Shenzhen, China). SiO_2/Si was supplied by Suzhou Institute of Nano-Tech and Nano-Bionics (SINANO) Chinese Academy of Sciences, China. The ROL-7133 stripped photoresist was supplied by Suzhou Rdmicro Limited Technology Company, China. Pb, H_2PtCl_6, PEG-400, isopropanol and hydrazine hydrate were provided by Sinopharm Chemical Reagent Co., Ltd., China.

1.2 Methods

1.2.1 Pt/graphene FET preparation

The schematic diagram of Pt/graphene sensor preparation is shown in Fig. 1. Firstly, graphene was prepared by using an optimized mechanical exfoliation method. Graphene was placed on a neutral-viscosity blue film with tweezers and repeatedly folded and pressed for 7–8 times. Then, the blue film was transferred onto a SiO_2/Si substrate (300 nm single-sided SiO_2 oxide layer), and heated on a heating table at 60 ℃ for 1 min. Graphene was peeled off from the blue film after it was cooled down. After the transfer was completed, the location of the graphene was marked. After the sample was heated at 100 ℃ for 1 min, the ROL-7133 stripped photoresist was spin-coated on the surface of the sample. After spin-coated, the sample underwent pre-baking, exposure, middle baking, development and glue removing. Then, the graphene FET was prepared by evaporating coatings with lift-off lithography. Finally, the Pt/graphene sensor was prepared by one-step reduction of Pt with the hydrazine hydrate.

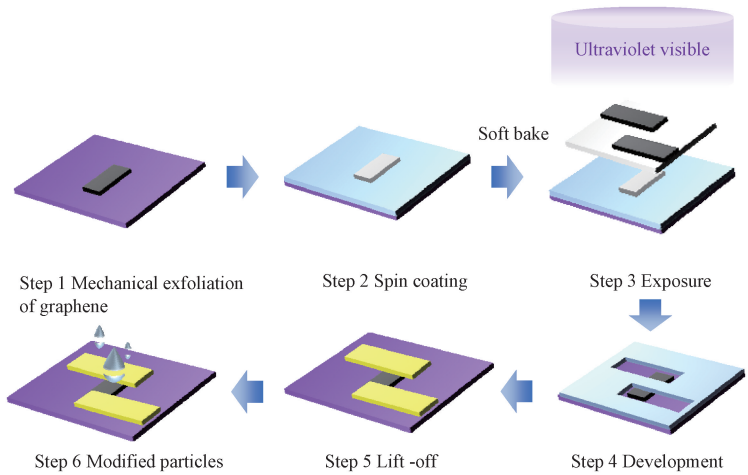

Fig. 1 Schematic diagram of Pt/graphene sensor preparation

1.2.2 Optimized glue removing method by isopropanol

The Pt/graphene sensor was held with tweezers, and the isopropanol was poured into the beaker and heated to 40 ℃ with magnetic stirring for 3 h. The residual gel on the surface of graphene was removed by isopropanol.

1.2.3 Surface functionalization of graphene

Hydrazine hydrate was used to reduce Pt in H_2PtCl_6 in one step. In order to control the size of the reduced Pt particles and to prevent the agglomeration of the Pt particles, PEG-400 was added as a dispersant. Firstly, the graphene FET sample treated with isopropanol was cleaned in a plasma cleaner (PDC-32G-2, Harrick Plasma, USA) with the power being selected as high-grade 18 W. The plasma-cleaned sample was taken out and immersed in 0.05 mmol/L H_2PtCl_6 for 3 h. Secondly, the experiment was configured with 10 mL hydrazine hydrate solution (a mass fraction of 10%). The dispersant PEG-400 (300 μL) was added with further ultrasonic for 10 min. Thirdly, 1 μL hydrazine hydrate solution was added dropwise to the graphene

surface. After a few seconds of reaction, the sample was rinsed slowly with isopropanol, and then slowly rinsed with deionized water to obtain the Pt/graphene sensor.

1.3 Characterization of Pt/graphene sensor

The morphology and electrical characterization of the Pt/graphene sensor were performed by an atomic force microscope (MFP-3D, Oxford Instruments, UK) and a source measurement unit (KEITHLEY 2612B, Tektronix, USA), respectively.

The feasibility of the optimized glue removing method by isopropanol was verified, and the Pt particles were characterized by a scanning electron microscope (S-4800, Hitachi, Japan) and energy dispersive spectroscope (AZtec X-Max^{N}80, Oxford Instruments, USA).

The electrical characteristics and resistance response of the Pt/graphene sensor were tested on a self-built source measurement unit gas detection platform. The high-precision CS200 flow controller and dynamic matching method were adopted, nitrogen was used as the carrier and hydrogen was used as the target gas. The gas flow rate was maintained at 3×10^2 cm^3/min, and the hydrogen volume fraction varied in the range of 0.08% to 0.12%.

The continuity test of the Pt/graphene sensor was done by continuously controlling the switching of the hydrogen output at a specific hydrogen volume fraction for sensitivity lifetime study. Firstly, before the test, nitrogen (5×10^2 cm^3/min) was injected for 300 s and the hydrogen volume fraction was maintained at 1.00%. The hydrogen input was stopped at 150 s and only the nitrogen input was turned on, till the end of the test before resuming nitrogen inject for 300 s, and so on for four cycles. By analyzing the relationship between the current response and the number of tests, we tested the Pt/graphene sensor for current and time variations over a fixed time period.

2 Results and Discussion

2.1 Sample characterization

Figure 2 shows the graphene surface morphology of the graphene FET by the atomic force microscopy (AFM). Isopropanol leaves a visibly adhesive residue on graphene that remains undissolved; nevertheless, the residual glue is reduced, and the adhesive is not dissolved. However, the residual glue on the surface has been reduced.

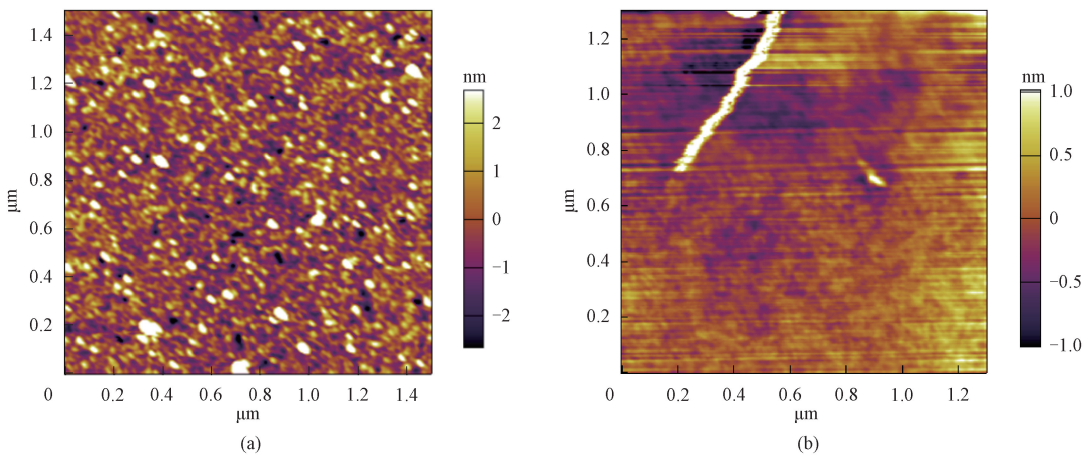

Fig. 2 Graphene surface tested by AFM: (a) before optimization; (b) after optimization by isopropanol

In order to further prove the effectiveness of the optimized glue removing method, the electrical properties of the sample were tested. The results of the electrical properties are shown in Fig. 3. The electrical properties of the sample are altered due to the presence of excess residual glue on the surface, resulting in decrease in the electrical conductivity. At a drain voltage V of 0, the drain current I is 2.51 μA. The presence of residual glue causes the surface doping of graphene, the I-V curve shifts to the left, and the linearity of the curve is greatly different, resulting in poor electrical properties. After optimization by isopropanol, the I-V curve is closer to the linear curve. At a drain voltage of 0, the drain current of the sample is 0.003 1 μA. The surface doping effect of graphene has been improved. The conductivity of the optimized sample is also improved and the linearity of the I-V curve slope has increased by 4.95 times.

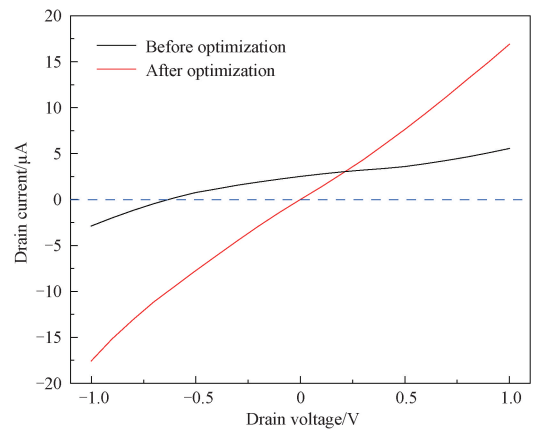

Fig. 3 Electrical properties of graphene FET before and after optimization

Pt element distribution and proportions of elemental contents tested by scanning electron microscopy (SEM) and energy dispersive spectroscopy (EDS) are shown in Figs. 4 (a) and 4 (b), respectively. The surface of graphene after plasma treatment is hydroxylated, and the binding ability of Pt particles to graphene is enhanced, making the distribution of Pt on the surface of graphene more uniform as shown in Fig. 4(a). The mass ratio of Pt to C is 3∶47, which is relatively high. Figure 4 (c) shows the surface morphology of the Pt/graphene sensor. The Pt particles are uniform in size and distribution.

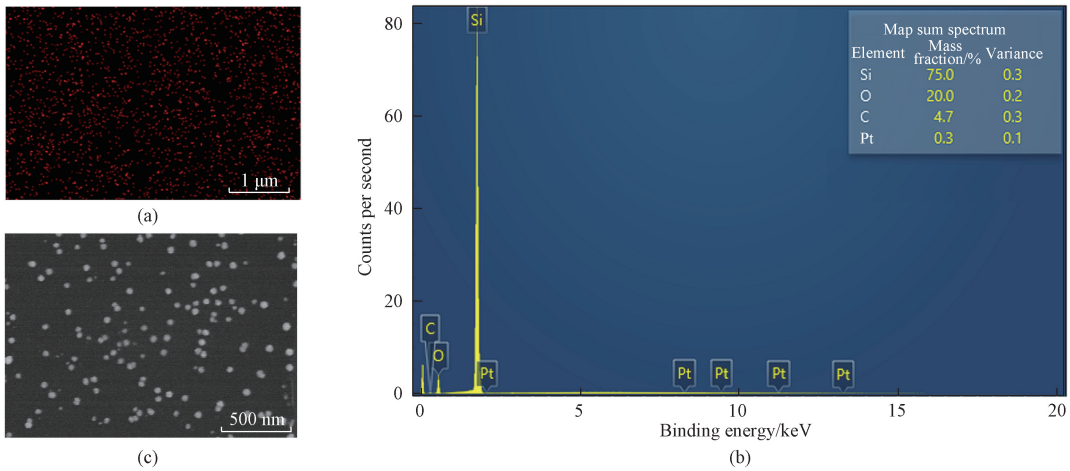

Fig. 4 SEM images and EDS results of Pt/graphene sensor: (a) Pt element distribution; (b) proportions of elemental contents; (c) Pt particle distribution

The *I-V* curves of the graphene FET and Pt/graphene sensor are shown in Fig. 5. The *I-V* curve of the graphene FET is almost straight. At the same drain voltage, the Pt/graphene FET has a substantial improvement in the absolute value of the current. According to Wang et al.[37], metal doping increases the electrical conductivity of graphene. The overlap of electron densities between C and Pt atoms is more obvious than that between C and C atoms, and the bonding ability between atoms is stronger. This shows that doped atoms can enhance electron transfer and improve conductivity. The band gap of the Pt/graphene sensor increases with the increase of the Pt mass fraction, which is beneficial to the conductivity of graphene.

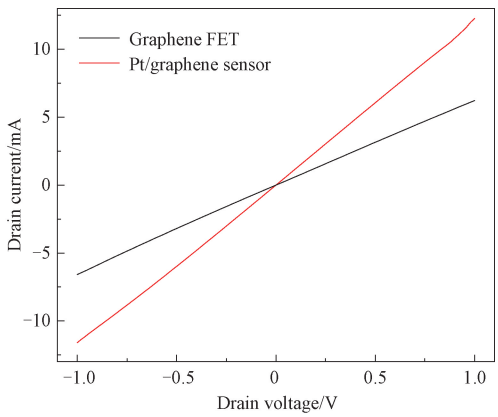

Fig. 5 Electrical property comparison of graphene FET and Pt/graphene sensor

2.2 Hydrogen detection by Pt/graphene sensor

As shown in Fig. 6, at different volume fractions of hydrogen, the resistance of the Pt/graphene sensor changes. When the hydrogen volume fraction is 0.08%, the resistance gradually decreases from the initial value of 3.9×10^4 Ω in the nitrogen to 2.9×10^4 Ω. When the hydrogen volume fraction increases to 0.10%, the resistance changes by 5.9% compared with that at a hydrogen volume fraction of 0.08%. When the hydrogen volume fraction continues to increase to 0.12%, the resistance changes by 18.0% compared that at a hydrogen volume fraction of 0.10%. When the hydrogen volume fraction increases to 0.08%, 0.10% and 0.12%, the resistance change rate reaches 25.73%, 30.13% and 42.72%, respectively. Thus, the resistance characteristics of the Pt/graphene sensor are different when detecting different volume fractions of hydrogen. It can be inferred that the Pt particles are selective in the hydrogen detection process.

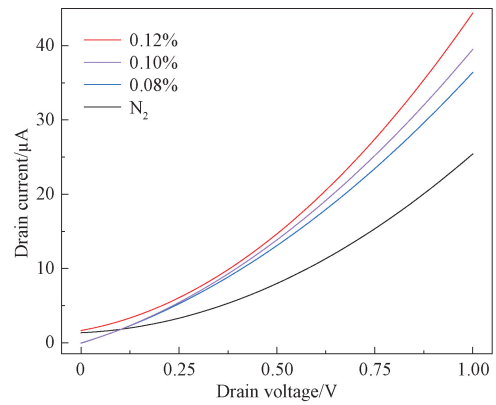

Fig. 6 *I-V* curves at different volume fractions of hydrogen

The resistance change rate is used to characterize the resistance response sensitivity of the sensor[38]. It is an important parameter to describe the response rate and stability of the sensor, and can dynamically reflect the resistance change of the sensor. The resistance response curves of the graphene FET and Pt/graphene sensor at a hydrogen volume fraction of 1.00% were compared and tested under constant conditions. As shown in Fig. 7, the graphene FET has low response to hydrogen. The resistance response curve of the Pt/graphene sensor is more pronounced, and after the introduction of hydrogen, the response curve peaks and stabilizes in a short period of time. Due to the limited hydrogen adsorption capacity of Pt, the volume ratio of hydrogen adsorption capacity of Pt is about 60∶1 to 70∶1. After saturation, a small amount of Pt also adsorbs hydrogen, and the resistance response curve fluctuates, but it is basically stable at about 30%.

Phan et al.[36] encapsulated the Pt/graphene sensor into a three-dimensional structure through the hydrothermal method. When the volume fraction of the hydrogen is 1.00%, the resistance change rate of the sensor is 15.1%. However, the measurement conditions of the sensing process require a high temperature of 200 ℃, which limits the application of the sensor. The Pt/graphene sensor prepared in this study operates at room temperature during the entire experiment process, and has a high resistance change rate to different hydrogen volume fractions. This further confirms the high sensitivity of Pt to hydrogen. When the hydrogen input is turned off, the response curve decreases significantly. However, due to the long time it takes for Pt to desorb hydrogen, the resistance response curve takes a long time to recover to 90% of the starting resistance. The results show that the Pt/graphene sensor is very sensitive to hydrogen.

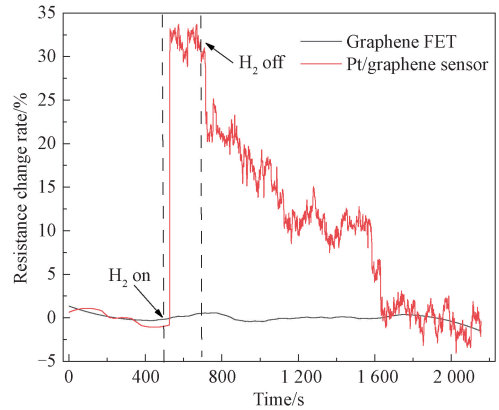

Fig. 7 Resistance response curves of graphene FET and Pt/graphene sensor at hydrogen volume fraction of 1.00%

The sensing characteristics at different hydrogen volume fractions of the Pt/graphene sensor and Pd/graphene sensor are compared as shown in Fig. 8. In Fig. 8(a), after hydrogen injection for 60 s, the resistance decreases significantly and begins to stabilize after reaching saturation with the peak resistance change rate of 20.97% and 33.35% at the hydrogen volume fraction of 0.80% and 1.00%, respectively. However, after reaching the peak, the resistance response curve fluctuates slightly, showing a certain degree of decline. After the hydrogen input is turned off, the resistance response curve decreases significantly, and the resistance begins to rise gradually and returns to the initial state.

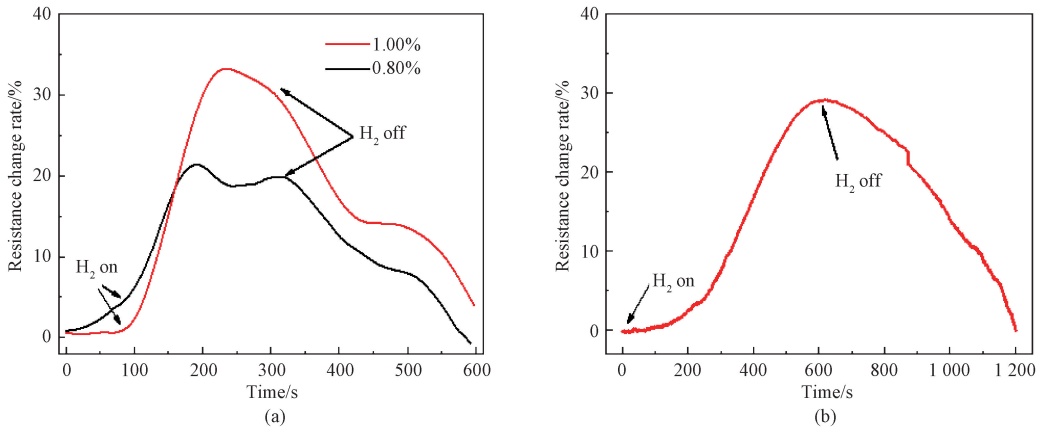

Fig. 8 Hydrogen resistance response curves: (a) Pt/graphene sensor; (b) Pd/graphene sensor

The Pd/graphene sensor was prepared using the same experimental method as that used in the previous preparation of the Pt/graphene sensor, and the same test method was used. The resistance response curve of the Pd/graphene sensor at a hydrogen volume fraction of 1.00% reaches the highest peak of 29.05% at about 600 s. The response time of the Pd/graphene sensor is higher than that of the Pt/graphene sensor.

Figure 9 illustrates a comparative plot of the current response of the Pt/graphene sensor at a fixed hydrogen volume fraction of 1.00%. In the first cycle, there is a large change in the current with a pronounced drop in the resistance and a rapid rise in the current. After reaching the set time for testing the hydrogen input, the hydrogen input is turned off, and the current falls rapidly. At the fourth cycle, the fluctuation of the current gradually

stabilizes and is accompanied by a certain hysteresis phenomenon. In order to further verify the effectiveness of the continuity test with a fixed hydrogen volume fraction, the peak resistance response rates of the four tests are compared, as shown in Fig. 9(b). From the continuity test results, the Pt/graphene FET releases hydrogen at a relatively slow rate, which adversely affects the subsequent hydrogen detection.

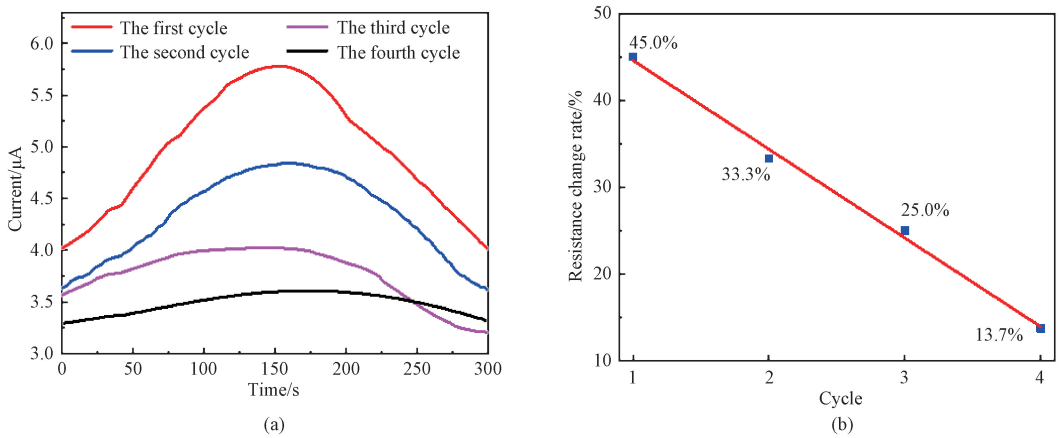

Fig. 9 Hydrogen continuous response: (a) current; (b) resistance change rate

2.3 Hydrogen detection mechanism of Pt/graphene sensor

The hydrogen adsorption of the Pt/graphene sensor include physical adsorption and chemical adsorption. The formation of hydrides affects the structure, bonding and strength between atoms, influencing the change in the resistance of the Pt/graphene sensor. In physical adsorption, hydrogen attaches to the surface of the Pt particles, decomposes into hydrogen molecules or atoms, and then interacts with the Pt particles through van der Waals forces. The chemical adsorption is a process in which dissociated hydrogen atoms bind to Pt particles via covalent bonds to form metal hydrides. The hydrogen sensor continuity test mechanism is shown in Fig. 10. During the cyclic hydrogen test, hydrogen atoms that are adsorbed on the Pt surface fail to desorb in time. Thus, as the number of tests increases, the resistance response rate shows a gradual downwards trend.

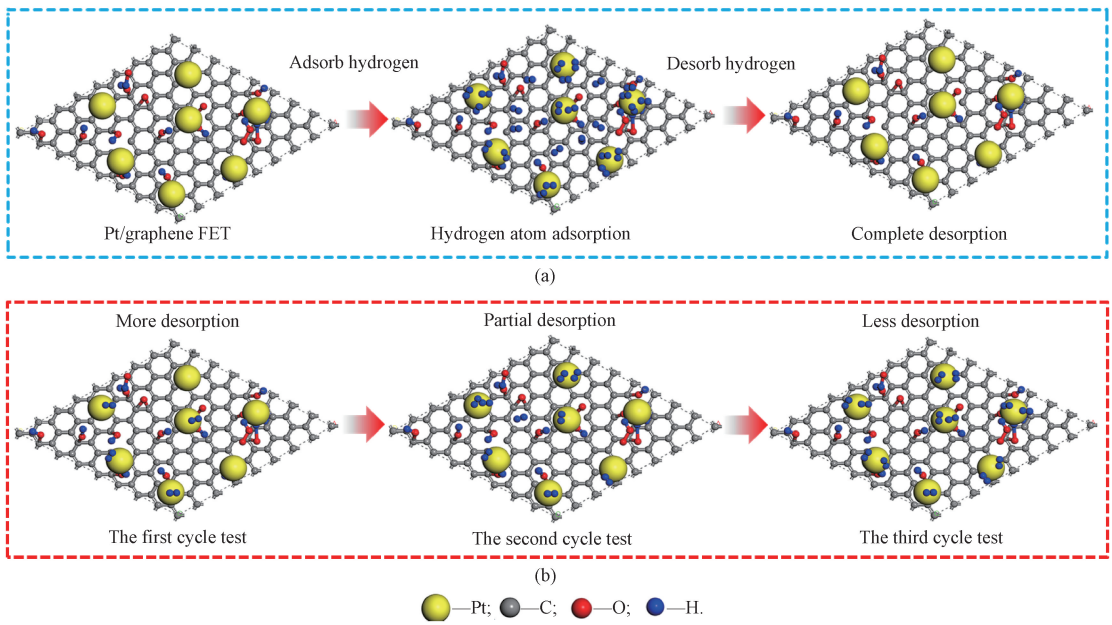

Fig. 10 Hydrogen sensor continuity test mechanism: (a) under ideal conditions with hydrogen being completely desorbed; (b) actual hydrogen atom desorption in different cycles

In the hydrogen adsorption process, hydrogen atoms are adsorbed on the Pt surface, and the Gibbs free energy of the adsorption reaction is positive, much higher than that of the desorption reaction. Hydrogen cannot be bound to Pt in the form of a molecule on the Pt surface, and it is easy to dissociate into hydrogen atoms[39]. The generation of Pt—H leads to a decrease of Pt and the migration of electrons from Pt—H to graphene. The rise

in the electron volume fraction enhances its conductivity and results in a decrease in the resistance of the hydrogen sensor. The overall can be described as

$$\text{Pt/graphene} + H_2 \longrightarrow \text{Pt/graphene-}H_2 \longrightarrow \text{Pt/graphene} + 2H \longrightarrow \text{Pt/graphene} + H_2. \quad (1)$$

Most of the Pt—H produced by the reaction can be stabilized[37]. Since Pt atoms form chemical bonds with hydrogen atoms, it takes a lot of energy to break these bonds. The desorption process is therefore relatively difficult and takes a long time. When saturation is reached, the time required for desorption exceeds the time required for hydrogen adsorption. Part of the Pt/graphene sensor surface is saturated in adsorption, and hysteresis in the sensor testing occurs in a confined environment with continuous hydrogen emission.

3 Conclusions

In this study, a Pt/graphene hydrogen detection sensor is successfully prepared by an optimized glue removing method by isopropanol. The conductivity of the optimized samples is also improved and the linearity of the *I-V* curve slope has increased by 4.95 times. The Pt/graphene sensor produced in this study has a high selectivity and sensitivity for hydrogen detection. The resistance characteristics are affected by the hydrogen volume fraction. The resistance response with Pt modification exhibits a higher sensitivity than that with Pd modification. The hydrogen chemical adsorption leads to a significant hysteresis during the continuity tests. Covalent Pt—H bonds make hydrogen desorption from the saturated surface slow and complex. This sensor shows a highly linearity of electrical properties. The findings would provide useful guidance for the rational design and further optimization of hydrogen sensors and promote its application in the aero-space industry.

References

[1] SOHAIL AHMAD M, INOMATA Y, KIDA T. Energy application of graphene based membrane: hydrogen separation[J]. *The Chemical Record*, 2024, 24(1): e202300163.

[2] JABALLAH S, DAHMAN H, GHILOUFI I, et al. Facile synthesis of Al-Mg co-doped ZnO nanoparticles and their high hydrogen sensing performances [J]. *International Journal of Hydrogen Energy*, 2020, 45(58): 34268-34280.

[3] LI Z, YAO Z J, ALI HAIDRY A, et al. Resistive-type hydrogen gas sensor based on TiO_2: a review[J]. *International Journal of Hydrogen Energy*, 2018, 43(45): 21114-21132.

[4] MIRZAEI A, YOUSEFI H R, FALSAFI F, et al. An overview on how Pd on resistive-based nanomaterial gas sensors can enhance response toward hydrogen gas[J]. *International Journal of Hydrogen Energy*, 2019, 44(36): 20552-20571.

[5] HÜBERT T, BOON-BRETT L, BLACK G, et al. Hydrogen sensors: a review[J]. *Sensors and Actuators B: Chemical*, 2011, 157(2): 329-352.

[6] LI X P, GU Z Y, CHO J, et al. Tin-copper mixed metal oxide nanowires: synthesis and sensor response to chemical vapors[J]. *Sensors and Actuators B: Chemical*, 2011, 158(1): 199-207.

[7] XIANG C L, ZOU Y J, QIU S J, et al. Nanocarbon-based materials for hydrogen sensor [J]. *Progress in Chemistry*, 2013, 25: 270. (in Chinese)

[8] LIU W L, CHEN C H, HAI W Q, et al. Laser-induced graphene conductive fabric decorated with copper nanoparticles for electromagnetic interference shielding application[J]. *Journal of Donghua University (English Edition)*, 2023, 40(6): 571-579.

[9] XIANG R F, CHEN X Y, LIU Y, et al. Porous graphene-based electrodes for fiber-shaped supercapacitors with good electrical conductivity [J]. *Journal of Donghua University (English Edition)*, 2023, 40(2): 134-141.

[10] ZHONG X J, LI W L, GAO X, et al. Preparation and output performance of triboelectric nanogenerator based on electrospun PVDF/GO composite nanfibers[J]. *Journal of Donghua University (Natural Science)*, 2024, 50(3): 15-22. (in Chinese)

[11] SCHEDIN F, GEIM A K, MOROZOV S V, et al. Detection of individual gas molecules adsorbed on graphene[J]. *Nature Materials*, 2007, 6: 652-655.

[12] WOLLANDT T, MANGEL S, KUSSMANN J, et al. Charging and electric field effects on hydrogen molecules physisorbed on graphene[J]. *The Journal of Physical Chemistry C*, 2023, 127(8): 4326-4333.

[13] FEDORENKO G, OLEKSENKO L, MAKSYMOVYCH N. Oxide nanomaterials based on SnO_2 for semiconductor hydrogen sensors[J]. *Advances in Materials Science and Engineering*, 2019, 2019: 5190235.

[14] CHOO T F, SAIDIN N U, KOK K Y. Hydrogen sensing enhancement of zinc oxide nanorods via voltage biasing[J]. *Royal Society Open Science*, 2018, 5(5): 172372.

[15] DEL ORBE D V, YANG H, CHO I, et al. Low-power thermocatalytic hydrogen sensor based on electrodeposited cauliflower-like nanostructured Pt black [J]. *Sensors and Actuators B: Chemical*, 2021, 329: 129129.

[16] TIAN J W, JIANG H C, ZHAO X H, et al. A Pb-level hydrogen sensor based on activated Pd

nanoparticles loaded on oxidized nickel foam[J]. *Sensors and Actuators B: Chemical*, 2021, 329: 129194.
[17] YANG Z H, DU X Q, YE X Q, et al. The free-standing nanoporous palladium for hydrogen isotope storage [J]. *Journal of Alloys and Compounds*, 2021, 854: 157062.
[18] NUGROHO F A A, DARMADI I, CUSINATO L, et al. Metal-polymer hybrid nanomaterials for plasmonic ultrafast hydrogen detection [J]. *Nature Materials*, 2019, 18: 489-495.
[19] ÖSTERGREN I, POURRAHIMI A M, DARMADI I, et al. Highly permeable fluorinated polymer nanocomposites for plasmonic hydrogen sensing[J]. *ACS Applied Materials & Interfaces*, 2021, 13(18): 21724-21732.
[20] YE Z, LI Z, DAI J X, et al. Hydrogen sensing performance investigations with optical heating and sensing element surface modification [J]. *International Journal of Hydrogen Energy*, 2021, 46(1): 1411-1419.
[21] DAS S, ROY S, BHATTACHARYA T S, et al. Efficient room temperature hydrogen gas sensor using ZnO nanoparticles-reduced graphene oxide nanohybrid[J]. *IEEE Sensors Journal*, 2021, 21(2): 1264-1272.
[22] SEO M H, KANG K, YOO J Y, et al. Chemo-mechanically operating palladium-polymer nanograting film for a self-powered H_2 gas sensor [J]. *ACS Nano*, 2020, 14(12): 16813-16822.
[23] PARK S, YANG J, LEE H M, et al. Effect of the position of amine groups on the CO_2, CH_4, and H_2 adsorption performance of graphene nanoflakes [J]. *Industrial & Engineering Chemistry Research*, 2023, 62(12): 5230-5240.
[24] LIU X L, YANG X M, CUI J W, et al. Ni coated with N-doped graphene layer as active and stable H_2 evolution cocatalysts for photocatalytic overall water splitting[J]. *ACS Catalysis*, 2023, 13(21): 14314-14323.
[25] JAISWAL J, DAS A, CHETRY V, et al. Vertically aligned porous V_xO_y nanofilms with Pt decoration for sub-ppm H_2 gas sensors[J]. *ACS Applied Nano Materials*, 2023, 6(4): 2646-2657.
[26] KOO W T, CHO H J, KIM D H, et al. Chemiresistive hydrogen sensors: fundamentals, recent advances, and challenges[J]. *ACS Nano*, 2020, 14(11): 14284-14322.
[27] YANG F, DONAVAN K C, KUNG S C, et al. The surface scattering-based detection of hydrogen in air using a platinum nanowire[J]. *Nano Letters*, 2012, 12(6): 2924-2930.
[28] NOVOSELOV K S, GEIM A K, MOROZOV S V, et al. Two-dimensional gas of massless Dirac fermions in graphene [J]. *Nature*, 2005, 438: 197-200.
[29] ZHANG Y B, TAN Y W, STORMER H L, et al. Experimental observation of the quantum Hall effect and Berry's phase in graphene[J]. *Nature*, 2005, 438: 201-204.
[30] POTYRAILO R A, SURMAN C, NAGRAJ N, et al. Materials and transducers toward selective wireless gas sensing [J]. *Chemical Reviews*, 2011, 111(11): 7315-7354.
[31] RUMYANTSEV S, LIU G X, SHUR M S, et al. Selective gas sensing with a single pristine graphene transistor[J]. *Nano Letters*, 2012, 12(5): 2294-2298.
[32] SINGH A K, UDDIN M A, TOLSON J T, et al. Electrically tunable molecular doping of graphene [J]. *Applied Physics Letters*, 2013, 102(4): 043101.
[33] RAD A S, PAZOKI H, MOHSENI S, et al. Surface study of platinum decorated graphene towards adsorption of NH_3 and CH_4 [J]. *Materials Chemistry and Physics*, 2016, 182: 32-38.
[34] CHEN D C, ZHANG X X, TANG J, et al. Adsorption and dissociation mechanism of SO_2 and H_2S on Pt decorated graphene: a DFT-D3 study[J]. *Applied Physics A*, 2018, 124(6): 404.
[35] HARLEY-TROCHIMCZYK A, CHANG J Y, ZHOU Q, et al. Catalytic hydrogen sensing using microheated platinum nanoparticle-loaded graphene aerogel[J]. *Sensors and Actuators B: Chemical*, 2015, 206: 399-406.
[36] PHAN D T, UDDIN A S M I, CHUNG G S. A large detectable-range, high-response and fast-response resistivity hydrogen sensor based on Pt/Pd core-shell hybrid with graphene[J]. *Sensors and Actuators B: Chemical*, 2015, 220: 962-967.
[37] WANG L L, LI W, CAI Y, et al. Characterization of Pt- or Pd-doped graphene based on density functional theory for H_2 gas sensor[J]. *Materials Research Express*, 2019, 6(9): 095603.
[38] LI H Y, WANG H L, WEI F Y, et al. Research progress of flexible wearable humidity sensors [J]. *Technical Textiles*, 2023, 41(9): 1-12. (in Chinese)
[39] HU S, TANG L J, ZHU Z H, et al. Dissociative adsorption study of hydrogen isotopes on metal platinum surface by thermodynamic computation [J]. *Journal of Atomic and Molecular Physics*, 2008, 25(2): 287-292. (in Chinese)

基于 Pt/石墨烯复合材料气体传感器的氢传感特性

侯天浩，彭倚天，丁树杨*
东华大学 机械工程学院，上海 201620

摘　要：石墨烯具有卓越的电学、光学和热学特性，可用于制备更薄、更轻和响应更快的传感器。该文在 SiO_2/Si 衬底上使用机械剥离方法制备石墨烯，并通过光刻法制备石墨烯场效应晶体管；通过水合肼还原法对石墨烯表面进行 Pt 颗粒修饰，以赋予 Pt/石墨烯传感器气敏特性；通过气体检测平台可获得不同氢气环境下的电学曲线和电阻响应曲线的特性。研究结果表明，Pt/石墨烯气体传感器在室温下对氢气表现出较高的灵敏度，在氢气体积分数为 1.00%时，电阻响应率高达 33.35%。然而在灵敏度寿命测试中发现，解吸过程存在本质滞后现象，这使得连续测试的电阻响应率出现明显下降。该文提供了一种基于石墨烯的气体传感器的改进制备方法，该方法将在航空航天中具有广泛的潜在应用。

关键词：石墨烯；Pt 颗粒；氢传感器；化学吸附